

Primljen/Received: 12.2.2016.

Ispravljen/Corrected: 18.5.2016.

Prihvaćen/Accepted: 11.8.2016.

Dostupno online/Available online: 10.10.2017.

Investigation of GFRP strengthened RC non-slender columns under eccentric loading

Authors:



Assist.Prof. **Gaurang R. Vesmawala**, PhD. CE
SVNIT - State Institute for Technology, India
Applied Mechanics Department
grv@amd.svnit.ac.in



Pradeep B. Kodag, MCE
SVNIT - State Institute for Technology, India
Applied Mechanics Department
pkodag@gmail.com

Scientific paper - Preliminary report

Gaurang R. Vesmawala, Pradeep B. Kodag

Investigation of GFRP strengthened RC non-slender columns under eccentric loading

An experimental analysis of reinforced-concrete columns was conducted in the paper to evaluate the effectiveness of circular, rectangular and square cross sections strengthened with the glass fibre reinforced polymer (GFRP) when subjected to eccentric loading. Parameters analysed in the paper are the type of cross section and eccentricity values. It was established that, due to uniform loading, the strength increase of circular sections is greater compared to square and rectangular sections. In addition, the strength and ductility of columns increase with the fibre reinforced polymer wrapping.

Key words:

ductility, eccentricity, column, glass fibre reinforced polymer (GFRP)

Prethodno priopćenje

Gaurang R. Vesmawala, Pradeep B. Kodag

Analiza ekscentrično opterećenih kratkih ab stupova ojačanih polimerom armiranim staklenim vlaknima

U radu je provedena eksperimentalna analiza armiranobetonskih stupova kako bi se odredila učinkovitost kružnih, pravokutnih i kvadratnih poprečnih presjeka ojačanih polimerom armiranim staklenim vlaknima (GFRP), pod utjecajem ekscentričnog opterećenja. Parametri koji se analiziraju su vrsta poprečnog presjeka i vrijednosti ekscentričnosti. Dobiveno je da se kod kružnih presjeka zbog jednolikog opterećenja postiže veće povećanje čvrstoće u usporedbi s kvadratnim i pravokutnim presjecima. Također se čvrstoća i duktilnost stupova povećavaju ojačanjem presjeka polimerom armiran vlaknima.

Ključne riječi:

duktilnost, ekscentričnost, stup, polimer armiran staklenim vlaknima (GFRP)

Vorherige Mitteilung

Gaurang R. Vesmawala, Pradeep B. Kodag

Analyse von exzentrisch belasteten kurzen GFK-verstärkten Stahlbetonsäulen

In der Arbeit wurde eine experimentelle Auswertung von exzentrisch belasteten Stahlbetonsäulen zur Prüfung der Effizienz von kreisförmigen, rechteckigen und quadratischen, glasfaserverstärkten Querschnitten durchgeführt. Die analysierten Parameter waren die Art des Querschnitts und der Wert der Exzentrizität. Es hat sich gezeigt, dass bei kreisförmigen Querschnitten infolge einer gleichmäßigen Belastung eine Steigerung der Festigkeit im Vergleich zu quadratischen und rechteckigen Querschnitten erreicht wird. Darüber hinaus steigen die Festigkeit und Duktilität der Säulen, deren Querschnitt mit einem GFK-verstärkten Polymer verstärkt wurde.

Schlüsselwörter:

Duktilität, Exzentrizität, Säule, glasfaserverstärkter Kunststoff (GFK)

1. Introduction

Repair, retrofitting and rehabilitation of existing structures have become a major part of construction industry due to various factors such as change in the use of structure, corrosion of reinforcement, poor quality construction, and change in loading conditions. Also, there is a need to upgrade the structures as per new design requirements. So, repair and retrofitting have been increasingly attracting attention of researchers all over the world during the past few decades.

The aim of this research is to study the effect of external fibre reinforced polymer (FRP) wrapping on columns under concentric loading. Columns with axial loading are rarely centric in practice. Columns are subjected to loading having eccentricity about single or both axes because of location of the column in plan, accidental loads, or bad workmanship. So there is a need to study the effect of eccentric loading on reinforced columns wrapped with FRP.

According to previous studies, circular cross section is the most effective cross section compared with square and rectangular cross sections. Circular shape offers good resistance to compressive loading because of hoop action. Square and rectangular cross-sections are subjected to stress concentration at their corners, leading to an ineffective confinement of the section, and finally resulting in a lower load carrying capacity. Therefore, the shape of column section plays a very vital role [1-3].

Rochette and Labossiere conducted a study on the increase in effectiveness of column confinement. They concluded that the corners of the columns with square and rectangular cross sections can be modified and chamfered, so as to avoid stress concentration and increase effectiveness of confinement and load carrying capacity. But there is a limitation to section chamfering because of presence of internal reinforcement in the RC section [2]. Ye et al. [4] observed that the shear strength of RC column can be effectively increased with external strengthening for columns wrapped with CFRP. Tamer El Maaddawy [5] conducted an experimental study of structural behaviour of the eccentrically loaded corrosion-damaged RC columns wrapped with carbon fibre reinforced polymer (CFRP) composites. The studies involving behaviour of columns wrapped with FRP composites under different eccentricities [6, 7], the use of different FRP sheets such as CFRP and E-glass fibre [8, 9], and a different number of FRP layers, were conducted by M. N. S. Hadi [10, 11]. A new stress-strain model for FRP-confined concrete columns was presented by You-Yi Wei and Yu-Fei Wu. This model can be used for general rectangular columns. In addition, it can be used for square columns when the cross-sectional aspect ratio, h/b , is equal to 1, and for circular columns when the corner radius ratio, $2r/b$, is equal to 1 [12]. A module for computing the stress-strain curve of the FRP confined concrete is given by Lam L. and Teng J. [13]. The finite element analysis carried out by A. Pravin and A. S. Jamwal demonstrates that the externally wrapped E-glass FRP constitutes a possible

solution for enhancing the strength and ductility of concrete specimens subjected to concentric loads. Parameters such as wrap thickness and ply configuration, as examined in the study, show that hoop-angle-hoop wrap configuration can be recommended [14]. Guoqiang L. et al. [15] have studied the effect of thickness, stiffness, and fibre orientation of FRP layers, as well as the interfacial bonding between the FRP wraps and concrete. Luke Bisby, et.al [16] present results of a test program relating to circular FRP-confined RC columns of realistic slenderness, subjected to eccentric axial loads. Test data are compared against theoretical P-M interaction diagrams, as well as against recently published design guidelines for P-M interaction in FRP-confined RC columns.

2. Axial compressive strength and maximum confining pressure

As per ACI 440.2R-08 [17], Eqns (1) and (2) are used to calculate the axial compressive strength of a non-slender, normal weight concrete member confined with an FRP jacket. For non-prestressed members with existing steel spiral reinforcement:

$$P_n = 0.85 [0.85f'_{cc}(A_g - A_{st}) + f_y \cdot A_{st}] \tag{1}$$

For non-prestressed members with existing steel-tie reinforcement

$$P_n = 0.8 [0.85f'_{cc}(A_g - A_{st}) + f_y \cdot A_{st}] \tag{2}$$

According to available literature, many axial compressive strength tests have been conducted on circular specimens, while just a small number of tests were conducted on non-circular reinforced concrete specimens confined with FRP. The existing strength model for FRP-confined concrete assumes the following form [9]:

$$\frac{f'_{cc}}{f'_{co}} = 1 + k_1 \left(\frac{f_1}{f'_{co}} \right) \tag{3}$$

where f'_{cc} and f'_{co} are compressive strengths of the confined and unconfined concrete, respectively, while k_1 is the confinement effectiveness coefficient. The confinement effectiveness coefficient k_1 is calculated according to Eq. (4) [18].

$$k_1 = 3.5 \left(\frac{f_1}{f'_{co}} \right)^{0.15} \tag{4}$$

$$f'_{cc} = f'_c + \Psi_f \cdot 3 \cdot k_a \cdot f_1 \tag{5}$$

$$f_1 = \left(\frac{2 \cdot E_f \cdot n \cdot t_f \cdot \epsilon_{fe}}{D} \right) \tag{6}$$

As per ACI 440.2R-08 [17], the maximum confined concrete compressive strength f'_{cc} and maximum confining pressure f_1 are calculated using Eqs. (5) and (6) with the inclusion of an additional reduction factor $\psi_f = 0.95$. The FRP strain efficiency factor k_ε may be taken as 0.55. For non-circular cross sections, f_1 in Eq. (5) and (6) corresponds to the maximum confining pressure of an equivalent circular cross section, with the diameter D equal to the diagonal of non-circular cross section (refer to Figure 1).

In Eq. (5), f'_c is the unconfined compressive strength of concrete cylinder, and the efficiency factor k_a accounts for geometry of the section, circular and non-circular. For circular cross sections, the shape factor k_a can be taken as 1. For non-circular cross sections, the shape factor k_a is calculated using Eq. (7) [17]:

$$k_a = \frac{A_e}{A_c} \left(\frac{b}{h} \right)^2 \quad (7)$$

In Eq. (6), the effective strain level in the FRP at failure ε_{fe} is given by,

$$\varepsilon_{fe} = k_\varepsilon \cdot \varepsilon_{fu} \quad (8)$$

$$D = \sqrt{b^2 + h^2} \quad (9)$$

Eq. (7), the ratio (A_e/A_c) is given by:

$$\left(\frac{A_e}{A_c} \right) = \left[\frac{1 - \frac{\left\{ \left(\frac{b}{h} \right) (h - 2r_c)^2 + \left(\frac{b}{h} \right) (b - 2r_c)^2 \right\}}{3A_g} - \rho_g}{1 - \rho_g} \right] \quad (10)$$

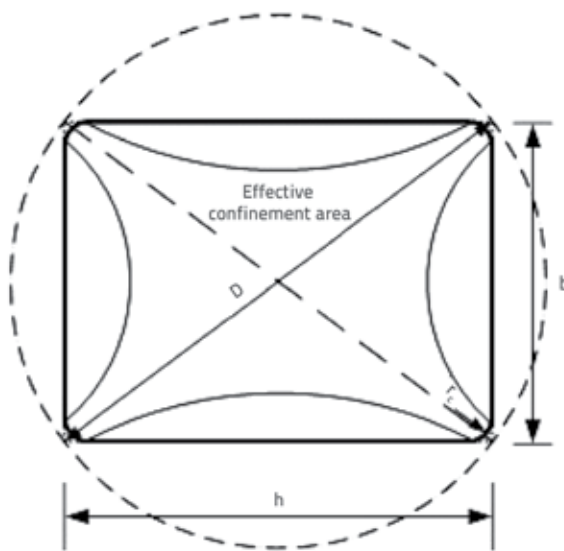


Figure 1. Equivalent circular cross section [17]

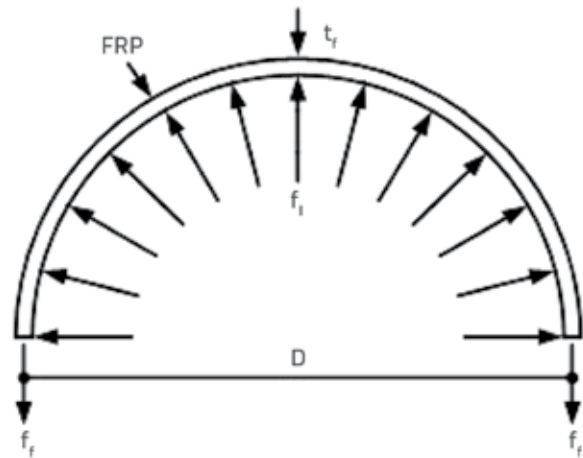


Figure 2. Lateral confining pressure exerted by FRP jacket

Notion:

- A_c - cross-sectional area of concrete in compression member [mm²]
- A_e - cross-sectional area of effectively confined concrete section, [mm²]
- A_g - gross area of concrete section [mm²]
- A_{st} - total area of longitudinal reinforcement [mm²]
- b - short side dimension of compression member of prismatic cross section [mm]
- D - diameter of compression member of circular cross section [mm]
- E_f - tensile modulus of elasticity of FRP [MPa]
- f'_c - unconfined compressive strength of concrete cylinder [MPa]
- f'_{cc} - compressive strength of confined concrete [MPa]
- f'_{co} - compressive strength of unconfined concrete [MPa]
- f_f - stress in FRP reinforcement [MPa]
- f_1 - maximum confining pressure due to FRP jacket [MPa]
- f_y - specified yield strength of non-prestressed steel reinforcement [MPa]
- h - long side cross-sectional dimension of rectangular compression member [mm]
- n - number of plies of FRP reinforcement
- P_n - nominal axial compressive strength of a concrete section [N]
- r_c - radius of edges of a prismatic cross section confined with FRP [mm]
- t_f - nominal thickness of one ply of FRP reinforcement [mm]
- ε_{fe} - effective strain level in FRP reinforcement attained at failure [mm/mm]
- ε_{fu} - design rupture strain of FRP reinforcement [mm/mm]
- ϕ - strength reduction factor
- k_a - efficiency factor for FRP reinforcement in determination of f'_{cc} (based on geometry of cross section)
- k_ε - confinement effectiveness coefficient
- k_1 - efficiency factor
- r_g - ratio of area of longitudinal steel reinforcement to cross-sectional area of a compression member
- ψ_f - FRP strength reduction factor

Table 1. Details of column specimens

Specimen ID	Strengthening	No. of layers of GFRP	Length [mm]	Shape of cross section	e_x [mm]	e_y [mm]
U(C/S/R)E0	Unwrapped	/	700	Circular/Square/ Rectangular	0	0
W(C/S/R)E0	GFRP wrapped	one	700		0	0
U(C/S/R)E30	Unwrapped	/	700		30	30
W(C/S/R)E30	GFRP wrapped	one	700		30	30
U(C/S/R)E40	Unwrapped	/	700		40	40
W(C/S/R)E40	GFRP wrapped	one	700		40	40

Note: U = unwrapped specimen; W = wrapped specimen; e_x, e_y = eccentricities along x-axis and y-axis, respectively; C = circular cross section; S = square cross section; R = rectangular cross section

3. Experimental investigation

3.1. Experimental program

The experimental research was carried out on circular, square and rectangular specimens externally wrapped with glass fibre sheets. Unidirectional glass fibre reinforced sheets were used with epoxy resin to glue the sheets externally around the reinforced concrete specimen. The properties of GFRP fibre and resin, as specified by the manufacturer, are presented in Table 2 and Table 3.

The parameters were investigated on a total number of 54 specimens cast in two stages. The first stage of testing involved 27 unwrapped specimens and the second stage involved 27 GFRP wrapped specimens. The testing was conducted using a universal testing machine. GFRP sheets were wrapped in the direction perpendicular to the longitudinal direction of the column. A gap of 5 mm was kept to avoid direct contact between the GFRP sheets and the loading machine.

General properties and dimensions of column specimens are shown in Table 1. For each group of 18 columns (i.e. circular, square, and rectangular), 6 columns were tested axially, 6 columns were tested with the 30 mm eccentric load, and 6 columns were tested with the 40 mm eccentric load.

3.2. Material properties

Tests were conducted to establish properties of the design mix for concrete, and the tensile strength of deformed steel and mild steel bars. Properties of the glass fibre reinforcement polymer (GFRP) and epoxy resin were adopted as per manufacturer’s specifications.

3.2.1. Concrete

The adopted concrete mix design proportion was 1:1.56:2.95, with the water cement ratio of 0.5. One cubic meter of concrete contained 360 kg of cement, 562 kg of fine aggregates and 1062 kg of coarse aggregates. The 28 days compressive strength of concrete ranged from 25 MPa to 27 MPa. A 75-80 mm slump was adopted for all specimens.

3.2.2. Reinforcement

The longitudinal reinforcement used in this study consisted of plain bars 10 mm in diameter. Transverse reinforcement i.e. stirrups consisted of plain bars 6 mm diameter. The bar spacing was 200 mm. The ultimate strength of longitudinal and transverse reinforcement amounted to 510-525 MPa and 275-285 MPa, respectively. Reinforcement details of circular,

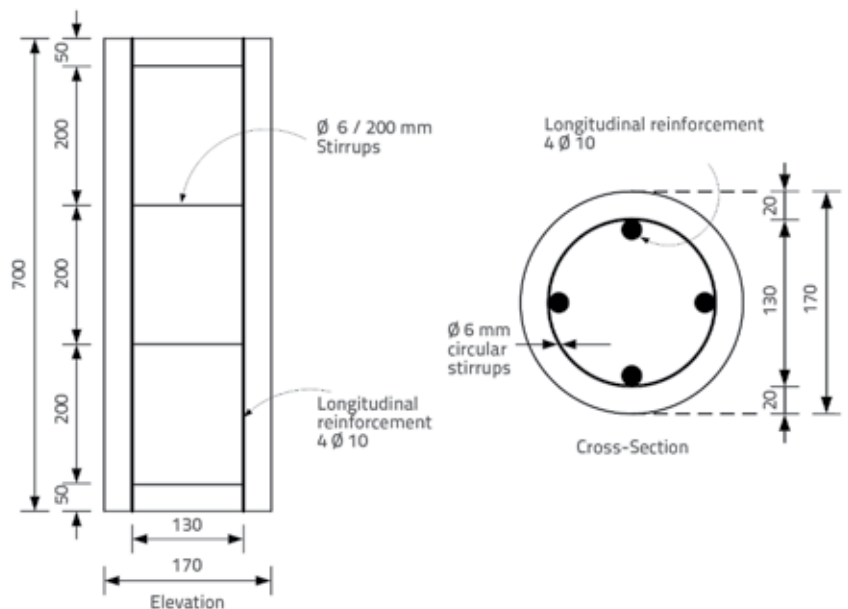


Figure 3. Reinforcement details for circular cross section

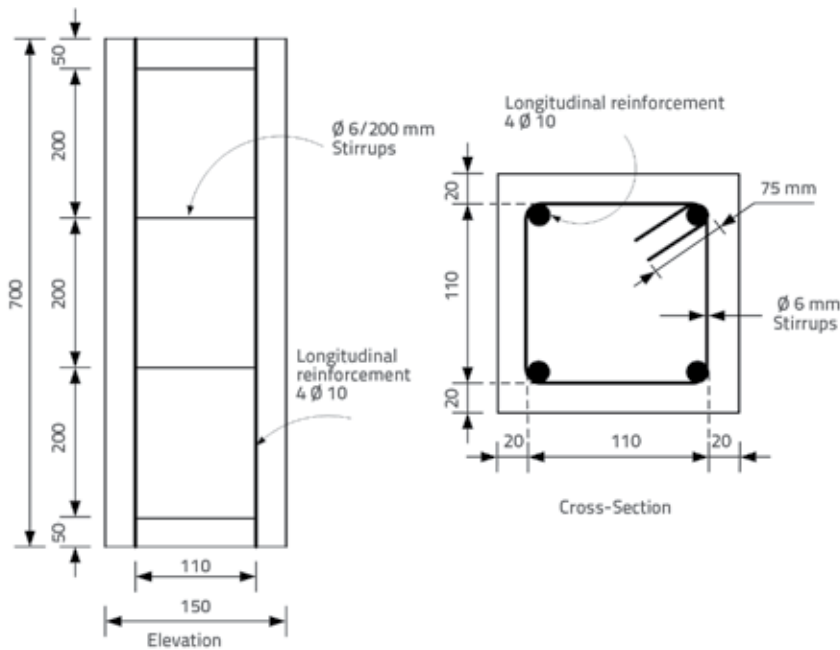


Figure 4. Reinforcement details for square cross section

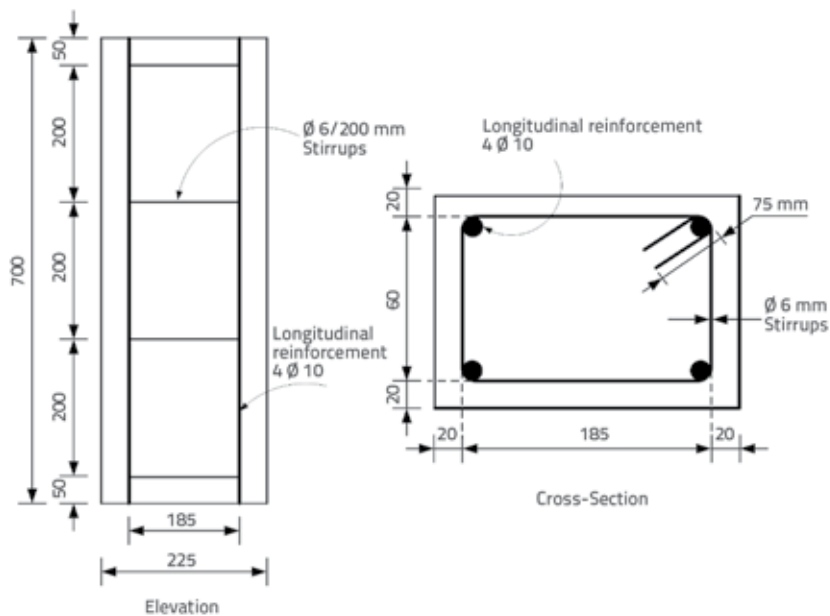


Figure 5. Reinforcement details for rectangular cross section

square and rectangular columns are shown in Figure 3, Figure 4, and Figure 5, respectively.

3.2.3. Glass fibre reinforced polymer and epoxy

Properties of the glass fibre reinforcement polymer (GFRP) and epoxy resin used in this study for external strengthening of reinforced concrete specimens are summarised in Table 2 and Table 3.

3.3. Preparation of specimens

The moulds for circular, square, and rectangular cross sections were custom made to ensure the quality work during casting of specimens, as the requirement differs from traditional ones. Two longitudinally cut cylindrical parts were used as moulds to easily remove the specimen from mould. Steel plates were welded at the top, middle and bottom of the moulds so as to ensure the same cross-sectional area of the specimen throughout the length (Figure 6). Specimens were removed from the moulds after 24 hours and cured for 28 days.

A total of 18 reinforced concrete columns were cast for each group of circular, square and rectangular cross sections. Three of each subgroup were kept as unwrapped specimens, and the remaining three were wrapped with a single layer of GFRP sheet. The formwork of square and rectangular specimens was prepared using a 18 mm thick plywood. Vertical sides and perpendicular edges of the corners

Table 2. Properties of fibres

Property	Fibres
Tensile strength [MPa]	2060
Tensile modulus [MPa]	75900
Specific gravity	2.56
Fibre thickness [mm]	0.43
Fibre orientation	Unidirectional
Elongation at break	0.04

Table 3. Properties of resin

Property	Resin
Tensile strength [MPa]	50
Tensile modulus [MPa]	3200
Elongation	5 %

were properly maintained in the mould assembly. After curing, corners of non-circular RC cross sections were chamfered with grinding machine so as to obtain a smooth contact surface. Putty was applied to smooth out rough corners. Obstructions were removed prior to FRP application. Plastic buckets were used for resin mixing. Typical mixing of the resin parts, with proper ratios, was carried out as per manufacturer's instructions. First, a primer was applied to the external concrete surface, and then resin putty was placed. Resin putty was used to fill small pores on the concrete surface. The first layer of the saturating resin was applied before complete curing of the primer and resin putty. A paint roller was used to apply the saturating resin in layers. The GFRP sheet was then carefully pushed into the saturating resin with a plastic roller in the hoop direction. The entrapped air was removed with the help of roller, which was followed by one more layer of saturating resin [19].



Figure 6. Moulds for circular columns

4. Instrumentation

The unwrapped and wrapped column specimens were tested using a universal testing machine with the load capacity of 2000 kN. The axial load on the column was recorded with the help of the UTM digital display. Axial and lateral deformations were

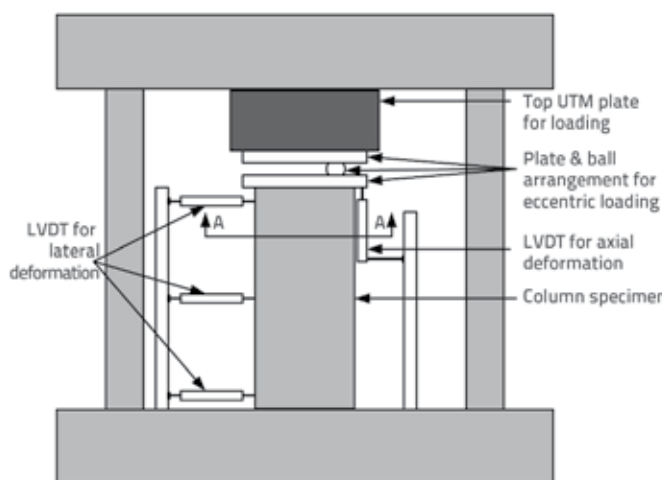


Figure 7. Instrumentation and test setup of column specimens

measured by means of linear variable differential transducers (LVDTs).

In case of eccentrically loaded columns, proper care was taken to apply the load at the desired location. Initially, a custom made steel plate was placed on the top surface of the specimen. The plate was levelled using levelling tube to avoid instrumental eccentricity. Special care was taken to avoid the contact of the bottom strip to the column specimen to ensure proper position of the plate on the specimen, and to make sure that no additional forces are exerted on the specimen during testing. A protection cage was provided around the specimen so as to avoid any damage to instruments or injury to persons working in the zone during the testing. A circular ring, with the diameter greater than the diameter of the column specimen, was provided at the bottom of the plate to avoid slippage of the plate from the column surface, without applying any additional forces to the specimen during testing. Figure 7 shows instrumentation and test setup of column specimens.

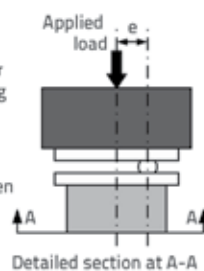
5. Experimental results and discussion

Experimental test results obtained in this study are given in Table 4 and Table 5. The applied load can be directly read from the electronic digital display of the universal testing machine. The deflections, both vertical and lateral ones, are recorded from the LVDT attached to the data acquisition system. The experimental ultimate load values and failure conditions are summarized in Table 5.

In this section, experimental results are expressed in terms of compressive load versus axial and lateral deformation values. Different modes of failure such as concrete crushing, FRP rupture, delamination of FRP sheet from the surface, spalling of concrete, and combined delamination and FRP rupture, may be expected. Two types of failure were mostly registered during this experimental study: concrete crushing, and rupture of GFRP reinforcements under hoop tension.

5.1. Behaviour of wrapped and unwrapped columns under axial load

All the columns were tested using universal testing machine, and subjected to constant load increment up to failure, with the load rate of 1kN/s. The performance of all the specimens was consistent under axial loading. The location of the rupture of the GFRP sheet for the axially loaded specimens was prominently at the top and bottom. Failure of unwrapped specimen was usual, with vertical cracks propagating on the surface, while a cracking noise



was heard in case of failure of confined specimens. This cracking noise signifies that the stress was transferred from bulged concrete to the GFRP jacket. The failure was steady and ended with a loud noise. A circumferential bulge was seen from all the sides of the specimen. For all specimens, failure was initiated by concrete crushing, and then the GFRP sheets were ruptured until the total failure of the specimen. The GFRP sheets were ruptured at a certain point, and then the cracks propagated upwards and downwards. A tremendous amount of energy was released with large explosive noise at the end showing that the FRP jacket provided a uniform confining action to the concrete core. As the load was gradually increased, the concrete gradually expanded before the GFRP ruptured. Delamination of the FRP sheet was rarely seen.

5.2. Behaviour of wrapped and unwrapped columns under eccentric load

The behaviour of eccentrically loaded specimens was quite different than that of the axially loaded specimens. Columns subjected to eccentric loading were subjected to both axial compressive loading and the moment created by force. The failure was evident by the bulking of the column in one direction. The load carrying capacity was observed to be lower than that of the axially loaded columns. It was very clearly evident that there was a decrease in the load carrying capacity of the column with an increase in the amount of eccentricity.

Buckling of the column was seen in the quadrant in which the load was applied. The failure noise was almost negligible for the confined columns, and a slight rupture was observed within the fibres. A failure pattern was observed in the unconfined column, but there was no significant change in confined columns. The GFRP laminates of failed specimens were not greatly damaged. Different failure modes are shown in Figure 8a-8d..

5.3. Load-deformation behaviour

The load-deformation behaviour of unconfined and GFRP confined specimens for circular, square, and rectangular cross sections, is presented in Figures 9- 11, respectively. The figures include the axial and lateral deformation obtained from LVDTs.

5.3.1. Axial loading

The performance of circular and non-circular specimens under axial load was consistent. An increase in the axial and lateral strain was observed with an increase in load. Cracking noise was heard prior to failure, indicating the start of stress transfer from dilated concrete to GFRP jacket. The load was increased at a constant rate until maximum load. The maximum load carrying capacity of unwrapped specimens at failure was 560 kN, 400 kN, 235 kN for circular, square, and rectangular specimens, corresponding to the deformation of 9.5 mm, 7.6 mm, and 6.8 mm, respectively.

5.3.2. Eccentric loading

The 30 mm and 40 mm eccentricity was applied to both unwrapped and GFRP wrapped specimens with the help of steel plate and ball arrangement. It is clear from the observations that there was a distinct decrease in the load carrying capacity of the specimens, as the eccentricity was introduced. Circular specimens showed a far better performance than the square and rectangular specimens. This is due to the fact that square and rectangular specimens were subjected to stress concentration at the corners against the hoop action for the circular specimens. In the plastic region, the load carrying capacity of circular specimens is greater compared to square and rectangular specimens.

Figure 9. Load-deformation response of circular specimens



Figure 8. Modes of collapse of columns: a) FRP rupture at circular column; b) FRP rupture at bottom corners; c) Spalling of concrete; d) Bulging effect

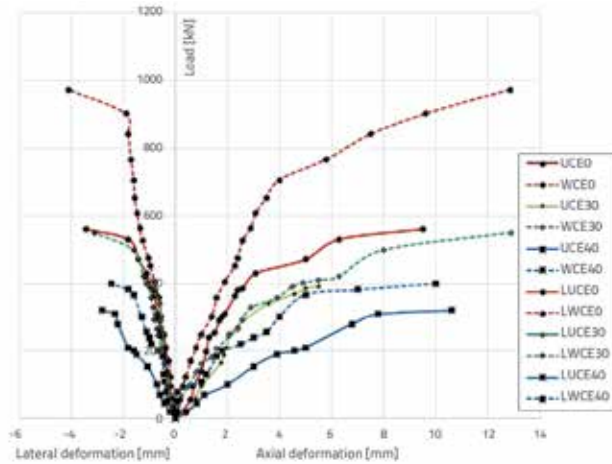
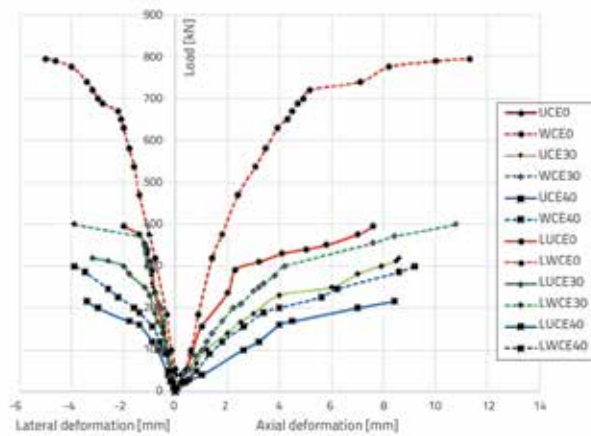


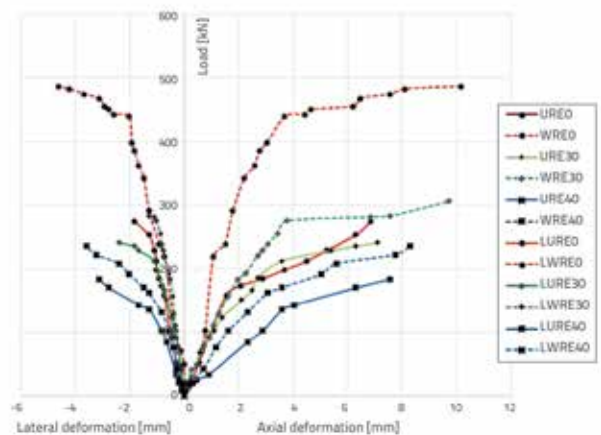
Figure 10. Load-deformation response of square specimens



In case of unwrapped specimens subjected to eccentric loading, specimen failure was initiated with concrete cracking in the quadrant in which the eccentric load was applied. Concrete spalling, leading to the end of the test, was observed. This resulted in the decrease in the load carrying capacity of the unwrapped specimens subjected to eccentric load. The prefix letter "L" used in legends of the Figures 9- 11 denotes lateral deformation. It can be seen from Table 4 that the maximum confining pressure

due to FRP jacket f_l is greater for a circular cross section, as compared to square and rectangular cross sections. The change in maximum confining pressure due to FRP jacket amounted to 20% for square cross section compared to a circular cross section, with the further difference of 13.75 % for rectangular cross section as compared to square cross section. The effective confinement ratio f'_{cc}/f'_{co} or maximum confinement pressure provided by FRP jacket is greater for circular cross section as compared to square and rectangular cross sections. This study also revealed a good agreement between theoretical and experimental results for both circular and square specimens, with maximum variation of 9 % for circular specimen. Experimental results for rectangular cross section showed variation of results of almost 40-50 % as compared to theoretical results. Thus, in case of rectangular cross sections the confinement was ineffective for the h/b ratio greater than 2.

Figure 11. Load-deformation response of rectangular specimens



5.3.3. Ductility

Ductility is one of important parameters of the FRP confined concrete columns. The value of ductility can be established by measuring the area under the load-deformation curve of the column specimen. For unwrapped axially loaded specimens,

Table 4. Effective lateral confinement pressure of FRP

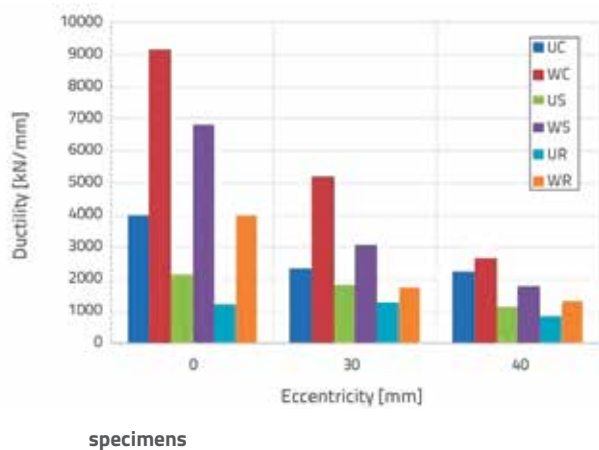
Cross section	Experimental			Calculation					$f'_{cc} \text{ (calculation)}/f'_{cc} \text{ (experimental)}$
	f'_{co}	f'_{cc}	f'_{cc}/f'_{co}	f_l	f_l/f'_{co}	k_1	f'_{cc}/f'_{co}	f'_{cc}	
Circular	25.85	42.82	1.66	3.08	0.119	4.82	1.57	40.07	0.94
Circular	25.69	43.73	1.70	3.08	0.120	4.81	1.58	39.88	0.91
Circular	25.77	43.35	1.68	3.08	0.120	4.81	1.58	39.97	0.92
Square	26.95	36.45	1.35	2.47	0.092	5.01	1.46	35.50	0.97
Square	25.85	35.07	1.36	2.47	0.096	4.98	1.48	34.21	0.98
Square	24.50	34.14	1.39	2.47	0.101	4.94	1.50	32.62	0.96
Rectangular	26.15	21.64	0.83	2.12	0.081	5.10	1.41	31.40	1.45
Rectangular	25.35	20.71	0.82	2.12	0.084	5.08	1.42	30.45	1.47
Pravokutni	25.80	21.06	0.82	2.12	0.082	5.09	1.42	30.98	1.47

Table 5. Summary of experimental results for all specimens

Specimen ID	GFRP failure point		Failure mode
	Load [kN]	Axial deformation [mm]	
UCE0	560	9.5	Peeling off concrete cover
WCE0	972	12.9	FRP rupture at mid-height with loud noise
UCE30	390	5.5	Peeling off concrete cover
WCE30	550	12.9	FRP rupture at mid-height with loud noise
UCE40	320	10.6	Peeling off concrete cover
WCE40	400	10	FRP rupture at mid-height with loud noise
USE0	395	7.6	Peeling off concrete cover
WSE0	795	11.3	Significant load drop & sound
USE30	321	8.5	Peeling off concrete cover
WSE30	400	10.8	Significant load drop & sound
USE40	216	8.4	Peeling off concrete cover
WSE40	300	9.2	Significant load drop & sound
URE0	235	6.8	Significant peeling off
WRE0	486	10.9	Significant load drop with little sound
URE30	272	7.6	Significant peeling off
WRE30	255	9.7	Significant load drop with little sound
URE40	183	7.5	Significant peeling off
WRE40	235	8.3	Significant load drop with little sound

the ductility of square and rectangular specimens decreased by 46 % and 69 %, respectively, compared to circular specimens. For GFRP wrapped axially loaded specimens, the ductility of square and rectangular specimens decreased by 26 % and 57 %, respectively, compared to circular specimens. Similarly, a decrease in ductility was also observed for the eccentrically loaded specimens. Thus, the square and rectangular cross-sectional shape and eccentricity of column specimens adversely affected the effectiveness of wrapping, which resulted in a decrease in ductility. This can be seen in Figure 12.

Figure 12. Ductility of unwrapped and GFRP wrapped column



6. Conclusion

A total of 54 RC non-slender column specimens (18 circular, 18 square and 18 rectangular specimens) were cast and tested under axial and eccentric compressive loading up to failure, in order to study the effect of cross section and eccentricity on the behaviour of FRP-confined columns. The following conclusions can be made from experimental investigations and comparison between different load and deformation values obtained from different eccentricities:

- Load carrying capacity of RC non-slender column can be significantly increased by wrapping the member externally with GFRP sheets. The external confinement with GFRP sheets considerably improved the load carrying capacity of specimens under axial loading, but the effectiveness faded out when eccentric load was applied on the specimen.
- The failure of all GFRP wrapped specimens occurred in a sudden and explosive way, and was preceded by a typical creeping sound. Collapse was mainly concentrated in their upper or lower portions.
- Because of a uniform hoop action, load carrying capacity of circular columns was by far better as compared to square and rectangular columns. The load carrying capacity of square and rectangular columns proved lower because of stress concentration at the corners, which was revealed by failure modes.

- External jacketing is a possible solution for increasing the strength and ductility of concentrically loaded specimens.
- The magnitude of eccentricity directly affected the maximum load carrying capacity. The larger the magnitude, the smaller the maximum load. External GFRP wrapping of RC non-slender columns resulted in large deformation without rupture.
- FRP jacket delamination was rarely registered. It can therefore be concluded that the provided overlap is sufficient to transferring load from concrete to FRP jacket.

REFERENCES

- [1] Mirmiran, A., Shahawy, M., Samaan, M., Echary, H.E., Mastrapa, J.C., Pico, O.: Effect of column parameters on FRP confined concrete, *ASCE Journal Composite Construction*, 2 (1998) 4, pp. 175-85, [https:// doi.org/10.1061/\(ASCE\)1090-0268\(1998\)2:4\(175\)](https://doi.org/10.1061/(ASCE)1090-0268(1998)2:4(175))
- [2] Rochette, P., Labossiere, P.: Axial testing of rectangular columns models confined with composites, *ASCE Journal Composite Construction*, 4 (2000) 3, pp. 129-36, [https:// doi.org/10.1061/\(ASCE\)1090-0268\(2000\)4:3\(129\)](https://doi.org/10.1061/(ASCE)1090-0268(2000)4:3(129))
- [3] Teng, J.G., Lam, L.: Compressive behaviour of carbon fibre reinforced polymer-confined concrete in elliptical columns, *ASCE Journal Structural Engineering*, 128 (2002) 12, pp. 1535-43, [https:// doi.org/10.1061/\(ASCE\)0733-9445\(2002\)128:12\(1535\)](https://doi.org/10.1061/(ASCE)0733-9445(2002)128:12(1535))
- [4] Ye, L., Yue, Q., Zhao, S., Li, Q.: Shear strength of reinforced concrete columns strengthened with carbon-fiber-reinforced plastic sheet, *ASCE Journal Structural Engineering*, 128 (2002) 12, pp. 1527-34, [https:// doi.org/10.1061/\(ASCE\)0733-9445\(2002\)128:12\(1527\)](https://doi.org/10.1061/(ASCE)0733-9445(2002)128:12(1527))
- [5] Tamer, El, M.: Post-repair performance of eccentrically loaded RC columns wrapped with CFRP composites, *Journal Cement and Concrete Composites*, 30 (2008), pp. 822-830, [https:// doi.org/10.1016/j.cemconcomp.2008.06.009](https://doi.org/10.1016/j.cemconcomp.2008.06.009)
- [6] Hadi, M.N.S.: Behaviour of Fibre RC Columns Wrapped with FRP under Eccentric Loads, *Australasian Structural Engineering Conference (ASEC)*, Melbourne, Australia, 26 - 27 June 2008.
- [7] Hadi, M.N.S.: Behaviour of FRP strengthened concrete columns under eccentric compression loading, *Composite Structures*, 77 (2007), pp. 92-96, [https:// doi.org/10.1016/j.compstruct.2005.06.007](https://doi.org/10.1016/j.compstruct.2005.06.007)
- [8] Hadi, M.N.S.: The behaviour of FRP wrapped HSC columns under different eccentric loads, *Composite Structures*, 78 (2007), pp. 560-566, [https:// doi.org/10.1016/j.compstruct.2005.11.018](https://doi.org/10.1016/j.compstruct.2005.11.018)
- [9] Li, J., Hadi, M.N.S.: Behaviour of externally confined high-strength concrete columns under eccentric loading, *Composite Structures*, 62 (2003), pp. 145-153, [https:// doi.org/10.1016/S0263-8223\(03\)00109-0](https://doi.org/10.1016/S0263-8223(03)00109-0)
- [10] Hadi, M.N.S.: Comparative study of eccentrically loaded FRP wrapped columns, *Composite Structures*, 74 (2006), pp. 127-135, [https:// doi.org/10.1016/j.compstruct.2005.03.013](https://doi.org/10.1016/j.compstruct.2005.03.013)
- [11] Hadi, M.N.S.: Behaviour of FRP wrapped normal strength concrete columns under eccentric loading, *Composite Structures*, 72 (2006), pp. 503-511, [https:// doi.org/10.1016/j.compstruct.2005.01.018](https://doi.org/10.1016/j.compstruct.2005.01.018)
- [12] Wei, Y.Y., Wu, Y.F.: Unified stress-strain model of concrete for FRP-confined columns, *Construction and Building Materials*, 26 (2012), pp. 381-392, [https:// doi.org/10.1016/j.conbuildmat.2011.06.037](https://doi.org/10.1016/j.conbuildmat.2011.06.037)
- [13] Teng, J.G., Jiang, T., Lam, L., Luo, Y.Z.: Refinement of a design-oriented stress-strain model for FRP-confined concrete, *Journal Composite Construction*, 13 (2009), pp. 269-78, [https:// doi.org/10.1061/\(ASCE\)CC.1943-5614.0000012](https://doi.org/10.1061/(ASCE)CC.1943-5614.0000012)
- [14] Azadeh, P., Aditya, S.J.: Effects of wrap thickness and ply configuration on composite-confined concrete cylinders, *Composite Structures*, 67 (2005), pp. 437-442, [https:// doi.org/10.1016/j.compstruct.2004.02.002](https://doi.org/10.1016/j.compstruct.2004.02.002)
- [15] Guoqiang, L., Samuel, K., Su-Seng, P., Helms, J.E.: Stubblefield, M., A.: Investigation into FRP repaired RC columns, *Composite Structures*, 62 (2003), pp. 83-89, [https:// doi.org/10.1016/S0263-8223\(03\)00094-1](https://doi.org/10.1016/S0263-8223(03)00094-1)
- [16] Luke, B., Michael, R.: Axial-flexural interaction in circular FRP-confined reinforced concrete columns, *Construction and Building Materials*, 24 (2010), pp. 1672-1681, [https:// doi.org/10.1016/j.conbuildmat.2010.02.024](https://doi.org/10.1016/j.conbuildmat.2010.02.024)
- [17] American Concrete Institute (ACI): Guide for the design and construction of externally bonded FRP systems for strengthening concrete structures, ACI-440.2R-08, Farmington Hills, MI, 2008.
- [18] Toutanji, H.A.: Stress-strain characteristics of concrete columns externally confined with advanced fibre composite sheets, *ACI Material Journal*, 96 (1999) 3, pp. 397-404.
- [19] Hayder, A.R.: *Strengthening Design of Reinforced Concrete with FRP*, CRC Press, Taylor & Francis Group, Boca Raton, Florida, U. S., 2014.